Nuclear Inst. and Methods in Physics Research, A 924 (2019) 256–261

Contents lists available at ScienceDirect

Nuclear Inst. and Methods in Physics Research, A

journal homepage: www.elsevier.com/locate/nima

The CMS Outer Tracker Upgrade for the HL-LHC

Alexander Dierlamm, on behalf of the CMS Tracker Collaboration

Institut für Experimentelle Teilchenphysik, Karlsruher Institut für Technologie, Hermann-von-Helmholtz-Platz 1, 76344 Egg.-Leopoldshafen, Germany

ARTICLE INFO

Keywords:
Silicon sensors
Tracking detector
Radiation hardness

ABSTRACT

The LHC is planning an upgrade program, which will bring the luminosity to about $5-7\times10^{34}$ cm^{-2} s^{-1} in 2026, with a goal of an integrated luminosity of 3000 fb^{-1} by the end of 2037. This High Luminosity LHC scenario, HL-LHC, will require a preparation program of the LHC detectors known as Phase-2 Upgrade. The current CMS Tracker is already running beyond design specifications and will not be able to cope with the HL-LHC radiation conditions. CMS will need a completely new Tracker in order to fully exploit the highly demanding operating conditions and the delivered luminosity. The new Outer Tracker system is designed to provide robust tracking as well as Level-1 trigger capabilities using closely spaced modules composed of silicon macro-pixel and/or strip sensors. Research and development activities are ongoing to explore options and develop module components and designs for the HL-LHC environment. The design choices for the CMS Outer Tracker Upgrade are discussed along with some highlights of the R&D activities.

1. Introduction to HL-LHC and the outer tracker upgrade of CMS

The Large Hadron Collider (LHC) at CERN will undergo an extensive upgrade program during the long shutdown 3 (2024–2026) to reach unprecedented performance. The instantaneous luminosity will reach 5–7$\times10^{34}$cm^{-2}s^{-1} and the integrated luminosity will reach 3000 fb^{-1} [1,2] (up to 4000 fb^{-1}, if the ultimate instantaneous luminosity can be achieved). As consequences of the increased LHC performance the detector has to cope with increased radiation levels and more collisions within one bunch crossing (pile-up, PU). The current trigger system of CMS [3] would not be capable of efficiently selecting the interesting events. It was shown that the track information from the tracking system can significantly improve the performance of the Level-1 (L1) trigger [4], which is the first instance of the trigger system. That necessitates to provide the relevant tracks for each bunch crossing. This is the main requirement that drives the layout and concepts of the new Outer Tracker for the HL-LHC phase. Further requirements and corresponding implementations are listed in Table 1.

2. Design of the new outer tracker for CMS

Fig. 1 shows the layout of the planned CMS Tracker. The Outer Tracker (radius r larger than 200 mm) contains only two types of modules, which are made of a stack of two silicon sensors with a gap of 1.6 to 4.0 mm depending on the position in the tracker. These modules, called 2S and PS modules, are specially designed to provide hits for each bunch crossing. The corresponding module concept, called p_T-module concept, is introduced in Section 3 and details of the module designs are given in Section 4.

The 13296 modules are arranged in barrel layers in the center and as double discs in the endcap regions. The inner barrel has a novel tilted geometry in the forward part for better tracking and reduced number of modules (i.e. lower material budget and costs), which is illustrated in Fig. 2. The temperature of the modules is controlled via two-phase CO_2 cooling (around −33 °C) being distributed with thin pipes also reducing the material budget. The electronic components on the modules are powered via DC–DC converters, which convert 11 V input voltage to the desired lower voltages. This reduces the required cable mass considerably.

The new tracker design and features allow for a reduced material budget and a better performance at high pile-up with respect to the current CMS tracker.

3. p_T-module concept, Track Finder and L1-trigger

The design of the modules is driven by the need of hit information for each bunch crossing. It is not possible to transfer all hit information to the back-end readout system and therefore, the module needs to select relevant hits thus reducing the amount of data being transmitted for each bunch crossing (while keeping all hit data in the readout chip buffers for a final trigger decision up to 12.5 μs later). This selection is performed by applying a cut on the transverse momentum of charged particles, which can be exploited in the high magnetic field of CMS.

E-mail address: alexander.dierlamm@kit.edu.

https://doi.org/10.1016/j.nima.2018.09.144
Received 29 January 2018; Received in revised form 21 September 2018; Accepted 26 September 2018
Available online 11 October 2018

Table 1
Requirements for the new CMS Tracker and their implementations followed by keywords being explained in this article.

Requirement	Implementation	Keywords
Operational up to 3000 fb^{-1}	Rad. resistance; cold operation (−20 °C)	n-in-p type silicon; CO_2 cooling
O(1%) occupancy up to PU≥140; robust pattern recognition	Increased granularity; optimized layout	Macro-pixel sensors
Contribute to L1 trigger	Track trigger capabilities	p_T-modules
Upgraded L1 trigger: higher rate (750 kHz), longer latency (12.5 μs)	Large readout bandwidth; deep front-end buffers	Binary readout; gigabit links
Reduce material effects	Optimization of passive volumes and services	CO_2 cooling; tilted barrel; DC–DC-powering

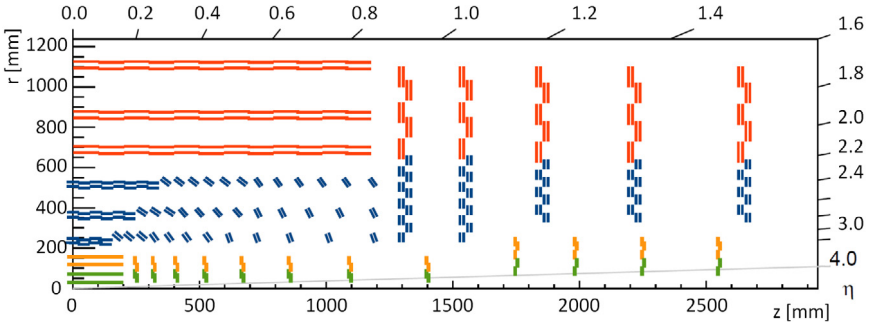

Fig. 1. Layout of the new CMS Tracker [5]. Shown is a quarter section of the tracker. 2S modules are indicated as red lines (r> 600 mm), PS modules as blue lines (200 mm<r< 600 mm). At lower radius and closer to the beam pipe is the pixel detector or Inner Tracker, which is not covered in this article. (For interpretation of the references to color in this figure legend, the reader is referred to the web version of this article.)

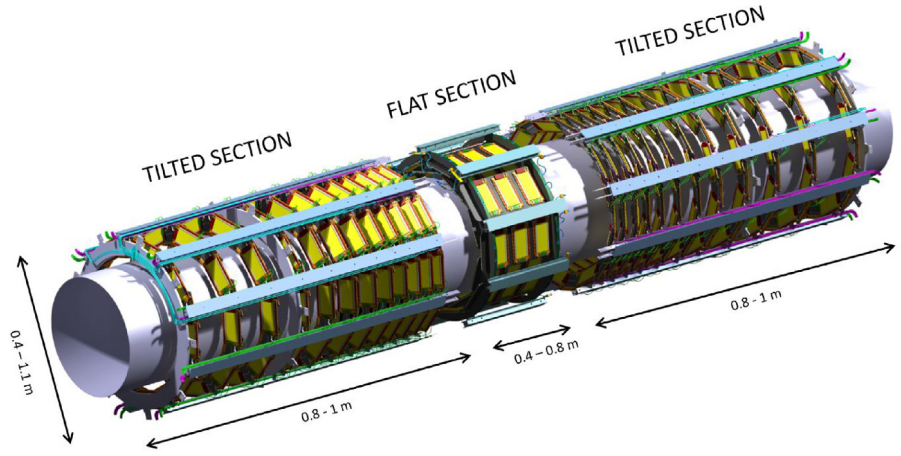

Fig. 2. Drawing of the innermost layer of the barrel section, showing the central flat section and the two (identical) tilted sections [5]. This layer also integrates the central part of the Inner Tracker support tube, as visible inside.

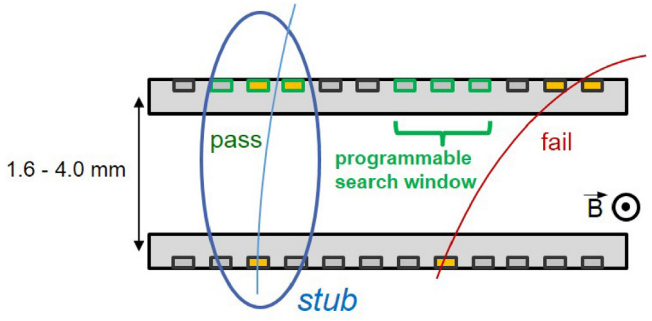

Fig. 3. Illustration of the identification of particles with high transverse momentum (p_T-concept). A hit in the lower sensor opens a programmable search window in the upper sensor such that particles with a momentum larger than about 2–3 GeV/c should pass through this sensor area. Such events are selected as trigger relevant data and shipped out as stubs.

A programmable search window allows to select straight, i.e. high transverse momentum (p_T), trajectories as illustrated in Fig. 3. A cut corresponding to 2 GeV/c already removes 99% of the particle tracks. The accepted short track segments including the position and bend information, referred to as stubs, are transferred to the back-end via high-speed optical links and further to the Data, Trigger and Control (DTC) system and Track Finder. In this path the data is processed and fitted track parameters are provided to the L1-trigger system within 4 μs. This massive computation task will be highly parallelized (time-multiplexing) and performed on many Track Finding Processors based on FPGAs as a reference system [5].

The p_T-module concept is realized in two module types, 2S and PS modules, described in the next section.

4. Module types and assembly

Each of the inner modules of the Outer Tracker consists of a single-sided **s**trip sensor and a **p**ixel sensor. These are called **PS** modules. The

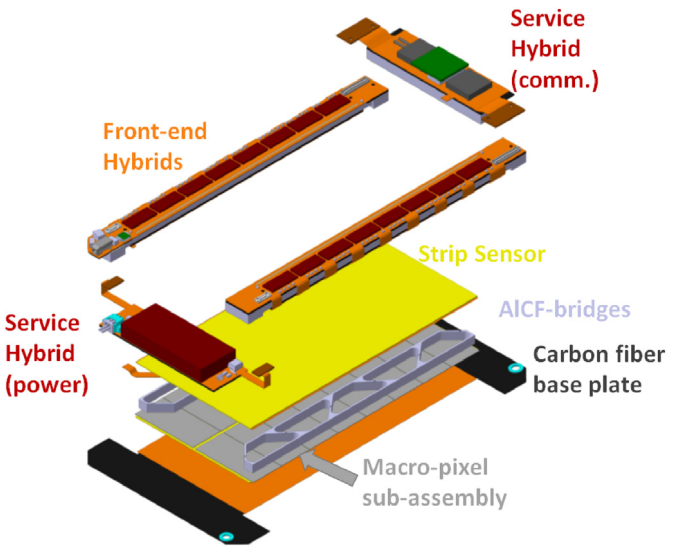

Fig. 4. Drawing of the PS module type. Shown is the exploded view of parts as they need to be assembled at the module assembly sites. The macro-pixel sub-assembly is the bump-bonded entity of macro-pixel sensor and 16 MPA readout chips.
Source: Adapted from [5].

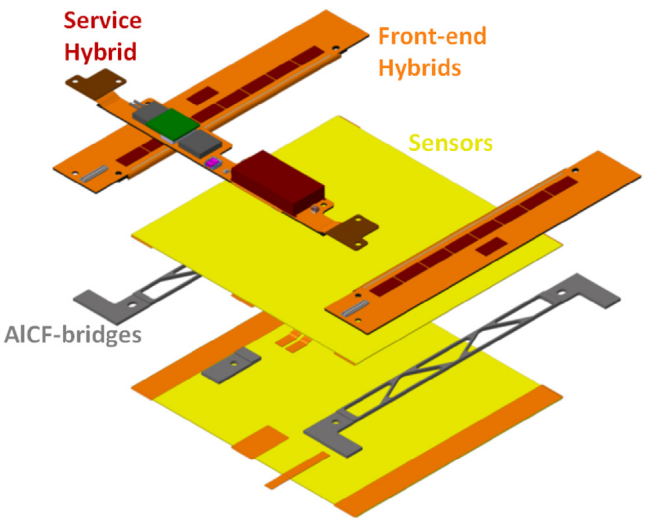

Fig. 5. Drawing of the 2S module type. Shown is the exploded view of parts as they need to be assembled at the module assembly sites.
Source: Adapted from [5].

strip sensors are segmented in two rows of 960 strips with pitch of 100 μm and length of 2.5 cm. The pixel sensors consist of 32 × 960 macro-pixels with size of 100 μm × 1.5 mm. This PS module type is illustrated in Fig. 4. The strip sensors of the PS module are connected to the strip sensor ASIC (SSA) [6], which sends hit information to the macro-pixel ASIC (MPA) [7], where the required correlation of hits in the upper strip sensor and the lower macro-pixel sensor is performed. These modules provide higher granularity due to the short macro-pixels, which is required for a good vertex resolution along the beam direction for L1-tracks. The expected maximum fluence for PS modules is $9.6 \times 10^{14}\ n_{eq}/cm^2$ after 3000 fb^{-1}. The **2S** modules consist of **2 s**trip sensors, which are segmented in two rows of 1024 strips with pitch of 90 μm and length of 5 cm (Fig. 5). The readout chips (CMS Binary Chip, CBC) [8] are connected to the upper and lower sensors via metal routing lines on the flex hybrid. The expected maximum fluence for 2S modules is $3 \times 10^{14}\ n_{eq}/cm^2$ after 3000 fb^{-1}.

Both module types contain all necessary readout (readout chips as well as aggregation and formatting stage) and service (power and communication) components and are operated as standalone readout entities.

A crucial aspect for both module types is the connection of the individual readout chips to both sensors. This is realized by flex Kapton® [9] hybrids bent around a stiffener providing bond pads on both sides and traces to connect to the bump bonded readout chips. This is illustrated in Fig. 6 for the 2S module, but the concept applies to both module types.

The assembly of such modules demands very high precision on the parallelism of the upper and lower sensor strips or pixel columns. An angle between the sensors would cause the programmed search window to move depending on the hit location along the strip. This in turn affects the p_T-resolution and deteriorates the efficiency of the p_T-discrimination for L1-tracks. The requirement on the angle between the upper and lower strips is set to 400 μrad for 2S modules (800 μrad for PS), and motivated by the fact that the strips should not deviate more than ±20 μm (less than half the pitch) along their length. Parallel offsets can be accounted for by configuring the chips accordingly and are not affecting the stub finding. The necessary sensor positioning accuracy is achieved by exploiting the good dicing precision (standard quality without requesting high accuracy) of the sensor manufacturers and assembly jigs with precision alignment pins. Methods to monitor the rotation between the upper and lower strips have been developed, which will also be used for quality control during production. One of such setups is described in more detail in [5].

Modeling of the thermal performance of these modules was used to optimize the mass of the spacers. These spacers are made of carbon fiber reinforced aluminum (AlCF [10]) for very good thermal conductivity and a coefficient of thermal expansion (CTE) well matched to silicon. The latter can be achieved by controlling the volume of carbon fibers leading to a combined CTE. The cooling strategy for the two module types is slightly different. While the 2S modules are fixed on five points to the cooling pipe via small cooling blocks, the PS modules are cooled via the whole back-surface of the macro-pixel sensor. This surface cooling is realized by gluing the bare module (macro-pixel sub-assembly and strip sensor glued to the AlCF spacers) to a heat spreading carbon-fiber baseplate, which in turn is glued to a large area cooling joint (Section 5.3).

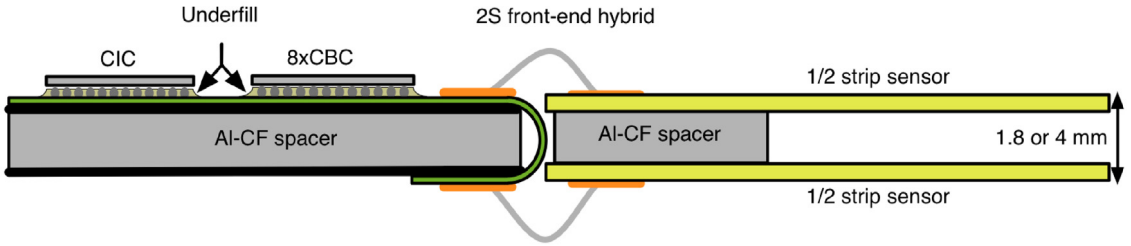

Fig. 6. Illustration of the electrical connectivity of the front-end hybrid to the sensors on the 2S module [5].

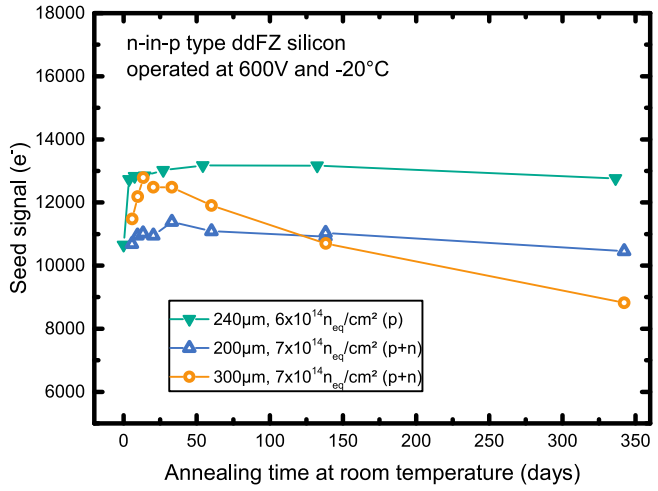

Fig. 7. Annealing of the seed signal (highest single strip signal in a cluster) for irradiated thick (300 µm) and thin (200 µm and 240 µm) sensors [5]. The annealing was performed at 60 °C and the duration is scaled to room temperature via the scaling factor of leakage current according to [11]. It is expected that 2S sensors accumulate a total of 3×10^{14} n_{eq}/cm^2 and sensors in the PS modules accumulate 1×10^{15} n_{eq}/cm^2. The tracker is expected to remain at room temperature during the year-end-technical-stops for two weeks, accumulating 140 days of annealing.

5. Examples from prototyping

This section shows examples of the ongoing developments and prototypes for the above introduced upgrade.

5.1. Sensors

Sensors with n-type electrodes in p-type silicon bulk were chosen as the baseline technology [12]. It was shown that proper strip isolation can be achieved by both p-stop and p-spray technologies. Irradiation studies with samples of different p-stop concentrations recommend a moderate implantation dose to reduce high field induced noise or breakdown effects [13].

Full-size 2S sensors have been produced with the baseline layout and characterized to meet the specifications. Strip sensors with active thicknesses of 200 µm, 240 µm and 300 µm were tested for their radiation hardness. The aims were a high signal over threshold and a stable annealing behavior. The latter was found for strip sensors with a thickness of 240 µm and below as shown in Fig. 7. The most probable value (MPV) of the signal distribution should be three times above the threshold to be highly efficient and the threshold should be set to about four times the noise to reduce the fraction of falsely identified hits to less than 10^{-4}. This results in a factor of twelve higher MPV of the signal compared to the noise figure of the readout chip with attached sensor.

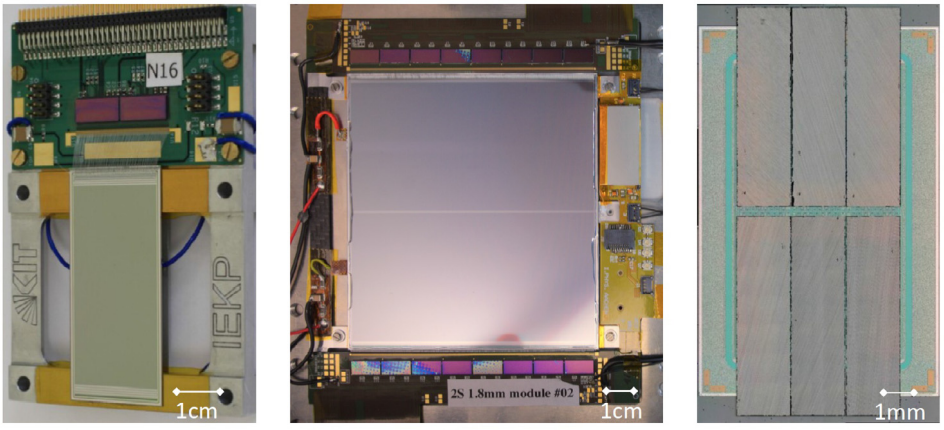

Fig. 8. Images of prototype modules [5]. From left to right: 2S mini module, full-size 2S module with prototype service hybrid, small macro-pixel sub-assembly with six chips.

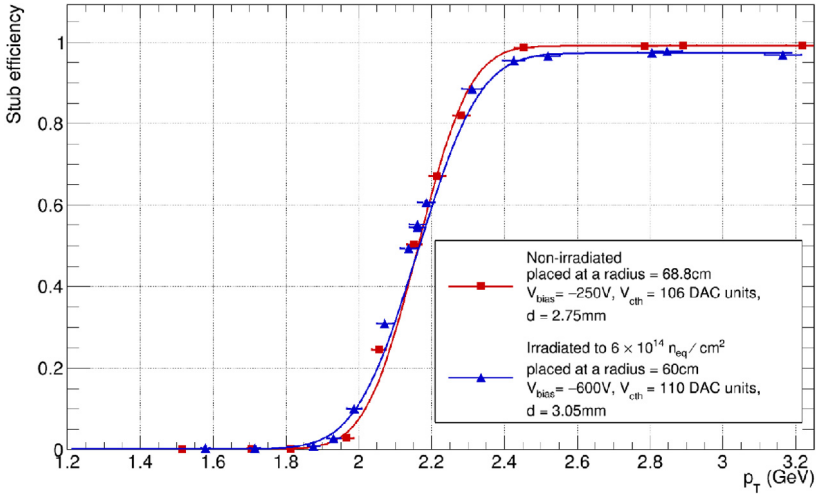

Fig. 9. Stub reconstruction efficiency for a non-irradiated (red) and an irradiated (blue) 2S mini-module [5]. The mini-module was irradiated to a fluence of 6×10^{14} n_{eq}/cm^2. The variable Vcth refers to the threshold setting, while d is the sensor spacing. Slightly different radii around 65 cm were used to calculate the momentum compensating for the fact that the modules had different sensor spacing but were operated with the same stub acceptance window. (For interpretation of the references to color in this figure legend, the reader is referred to the web version of this article.)

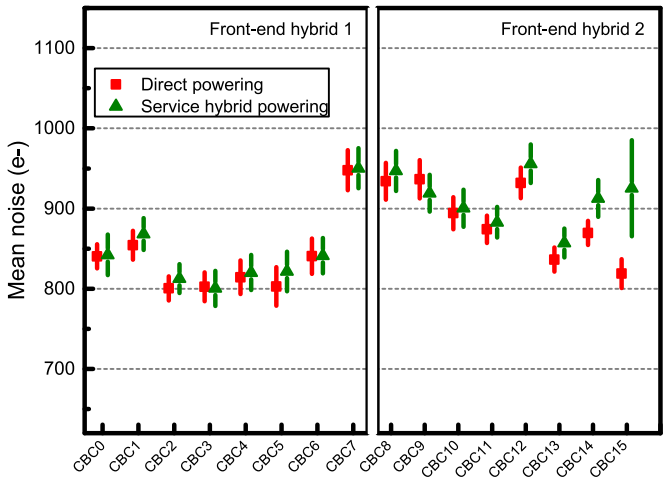

Fig. 10. Average noise values for the 16 CBCs on both hybrids of a 2S module. The power was either provided directly from the lab power supply (red) or via the DC–DC converter on a prototype service hybrid (green). CBC15 is closest to the shielded air coils of the DC–DC converter, for which the position is representative of the final design (upper right CBC in Fig. 8 center). (For interpretation of the references to color in this figure legend, the reader is referred to the web version of this article.)
Source: Adapted from [5].

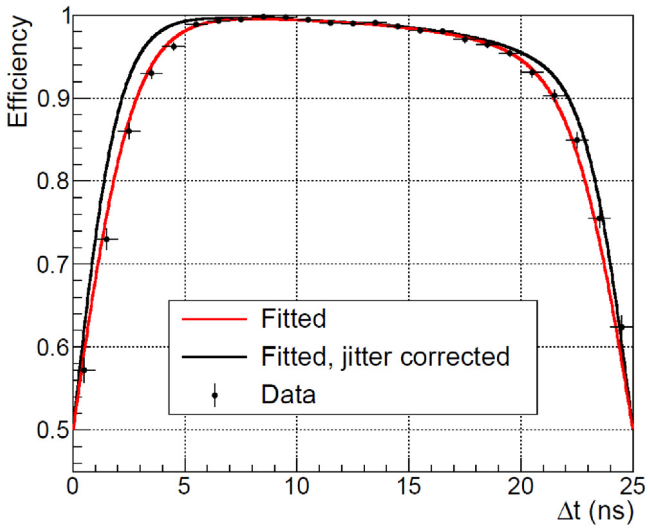

Fig. 11. Efficiency of the hit identification with a small macro-pixel sub-assembly prototype [5]. The efficiency is plotted versus the trigger arrival phase. The timing jitter in the system was determined and the profile was deconvoluted accordingly.

For the signal distribution the seed signal is chosen, which is the highest single strip signal in a signal cluster. This is more representative when applying a readout threshold. Sensors for 2S modules are required to provide a signal of 12 000 electrons due to a noise of about 1000 electrons. The strip sensors of the PS modules are read out by the SSA chip [6], which has about 700 electrons noise when connected to a 2.5 cm long strip and therefore the signal should exceed 8400 electrons. For macro-pixel sensors a 4000 electrons signal is sufficient. Therefore, the current baseline is 240 μm for strip sensors and 200 μm for macro-pixel.

5.2. Modules

A first prototype module for the demonstration of stub finding was assembled from two small sensor prototypes and a rigid front-end hybrid containing two CBC chips of version 2. The sensors have 256 5 cm long strips at 90 μm pitch and the sensors' back-to-back distance is about 3 mm. Such modules (Fig. 8 left) were tested in a particle beam at CERN SPS and DESY. They were placed inclined to the particle beam direction to produce tracks of different angles emulating the bending of the particles in the detector's magnetic field. Fig. 9 demonstrated that the stub finding works efficiently before and after irradiating the modules to about double the expected fluence. Finally, full-size 2S modules (Fig. 8 center) were assembled and characterized in particle beams at CERN SPS and FNAL confirming good uniformity of the hit detection efficiency over the module width.

Such a large module was also used to study the influence of the DC–DC powering with a prototype service hybrid containing shielded air coils as inductors. Fig. 10 shows that the noise of the closest CBC increased slightly compared to direct powering but stayed below the specified 1000 electrons.

Also a small version of the macro-pixel sub-assembly was designed and several assemblies produced. It consists of six small macro-pixel ASICs bump bonded to a miniature macro-pixel sensor (Fig. 8 right). They were successfully operated at test beams and show, as indicated in Fig. 11, very high efficiency in a wide window of the clock phase.

5.3. Mechanics

The tilted geometry for the inner layers housing PS modules and providing large area cooling joints for this module type represents a major challenge for mechanical design. The inner barrel layers are grouped in ring structures, which provide cold surfaces on which the modules can be glued (Fig. 12).

In the endcaps the cooling joints are embedded in the carbon-fiber sheets. A small prototype section was produced to learn about the manufacturing process and to study the transition region between the inner region populated with PS modules and the outer region populated with 2S modules. This prototype was also used to study the thermal performance of the design.

5.4. Track Finder

Track finding for each bunch crossing has several requirements for which the most important are:

- processing time window of 4 μs,
- transverse momentum resolution of about 2%,
- longitudinal vertex position resolution of about 1 mm,
- a significant rate reduction of 1/100.

The implementation of these requirements was demonstrated in hardware by three approaches [5]. All of them are organized in four processing stages: data organization, pattern recognition, track fitting and duplicate removal. The data is grouped in regions and the hardware multiplied for time-multiplexing. One approach also uses associative memory chips for the pattern recognition [14], while the other two are purely based on FPGA processing [15,16]. The latter have been chosen to be further developed on common hardware to optimize the FPGA-only reference system [5].

6. Conclusion and outlook

All the new concepts of the upgraded CMS Tracker have been validated and the corresponding Technical Design Report was approved by December 2017 [5]. The community will increase the quantity of prototypes to finalize the assembly processes and to allow more intensive system and integration tests. The quality assurance for all parts is being reviewed and quality control mechanisms will be detailed within the next two years.

The prototyping phase will continue with focus on large-scale production until pre-series productions are launched around 2020–2021. The installation and commissioning of the final detector is foreseen for 2025.

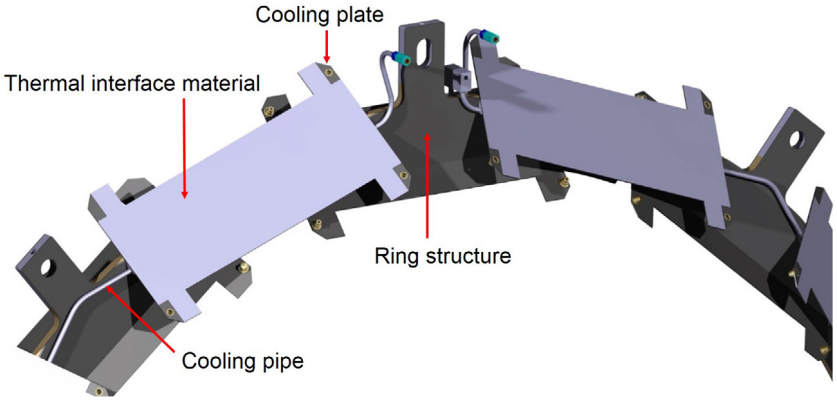

Fig. 12. CAD drawing of the tilted ring geometry including cooling pipe routing and cooling plates [5].

References

[1] http://hilumilhc.web.cern.ch/about/hl-lhc-project.

[2] I. Bejar Alonso, L. Rossi, HiLumi LHC Technical Design Report, CERN-ACC-2015-0140, 2015. https://cds.cern.ch/record/2069130.

[3] CMS Collaboration, The CMS experiment at the CERN LHC, J. Instrum. 3 (2008) S08004.

[4] CMS Collaboration, Technical Proposal for the Phase-II Upgrade of the CMS Detector, CERN-LHCC-2015-010, 2015. https://cds.cern.ch/record/2020886.

[5] CMS Collaboration, The Phase-2 Upgrade of the CMS Tracker, CERN-LHCC-2017-009, 2017. https://cds.cern.ch/record/2272264.

[6] K. Kloukinas, et al., Short-Strip ASIC (SSA): A 65 nm Silicon-Strip Readout ASIC for the Pixel-Strip (PS) Module of the CMS Outer Tracker Detector Upgrade at HL-LHC, PoS(TWEPP-17)031.

[7] D. Ceresa, et al., A 65 nm pixel readout ASIC with quick transverse momentum discrimination capabilities for the CMS Tracker at HL-LHC, J. Instrum., 11 (2016) C01054.

[8] D. Braga, et al., CBC2: A microstrip readout ASIC with coincidence logic for trigger primitives at HL-LHC, J. Instrum. 7 (2012) C10003.

[9] http://www.dupont.com/products-and-services/membranes-films/polyimide-films/brands/kapton-polyimide-film.html/.

[10] S. Seshan, A. Guruprasad, M. Prabha, A. Sudhakar, Fibre-reinforced metal matrix composites – a review, J. Indian Inst. Sci. 76 (1996) 1–14, http://journal.library.iisc.ernet.in/index.php/iisc/article/viewFile/2575/4137.

[11] M. Moll, Radiation Damage in Silicon Particle Detectors (Ph.D. thesis), University of Hamburg, 1999, DESY-THESIS-1999-040.

[12] A. Dierlamm, et al., P-type silicon strip sensors for the new CMS Tracker at HL-LHC, J. Instrum. 12 (2017) P06018.

[13] M. Printz, P-stop isolation study of irradiated n-in-p type silicon strip sensors for harsh radiation environments, Nucl. Instrum. Methods Phys. Res. A 831 (2016) 38–43.

[14] A. Rossi, et al., A Track Finder with Associative Memories and FPGAs for the L1 Trigger of the CMS experiment at HL-LHC, this issue.

[15] I. Tomalin, et al., An FPGA based track finder for the L1 trigger of the CMS experiment at the High Luminosity LHC, J. Instrum. 12 (2017) P12019.

[16] M. Zientek, et al., FPGA-Based tracklet approach to level-1 track finding at CMS for the HL-LHC, EPJ Web Conf. 150 (2017) 00016.